Predicting implant UHMWPE wear *in-silico*: A robust, adaptable computational-numerical framework for future theoretical models

M.A.Strickland[1]*, M.R.Dressler[2], M.Taylor[1]

[1] Bioengineering Sciences Research Group, University of Southampton, Hampshire, SO17 1BJ (UK)

[2] DePuy Orthopaedics, 700 Orthopaedic Drive, Warsaw, IN 46581-0988 (USA)

**Corresponding author e-mail: ams05@alumni.soton.ac.uk*

Co-author e-mail: mdressle@its.jnj.com, m.taylor@soton.ac.uk

Abstract:

Computational methods for the pre-clinical wear prediction for devices such as hip, knee or spinal implants are valuable both to industry and academia. Archard's wear model laid the basis for the first generation of theoretical wear estimation algorithms, and this has been adapted to account for the importance of multi-directional sliding. These second-generation cross-shear algorithms are useful, but they leave room for improvement.

In this paper, we outline a generalised framework for a 'third generation' wear model. The essential feature of this proposed approach is that it removes the acausality and scale-independence of current second-generation algorithms. The methodology is presented in such a way that any existing second-generation model could be adapted using this framework. Using this approach, the predictive power against pin-on-disc and implant tests is shown to be improved; however, the model is still essentially a purely adhesive-abrasive wear predictor, accounting for only a limited number of factors as part of the tribological process. Further ongoing work is needed to expand and improve upon the current capabilities of *in-silico* UHMWPE wear prediction capabilities.

Key Words:

Bio-tribology, UHMWPE Wear, Computational Modelling, Wear Theories

Introduction:

Implant wear is a key factor in the pre-clinical design of orthopaedic devices such as hip, knee, and spinal prostheses. Wear is a complex process, with multiple mechanisms (e.g. adhesive, abrasive, three-body and fatigue wear) and many influential factors (kinematics, stresses, chemical

environment, temperature), all resulting in a range of possible biological implications (e.g. different biological responses to different debris morphology [1]). It is highly valuable for both the industrial bioengineer and the academic researcher to have available a baseline predictive tool for qualitatively (and ideally, quantitatively) anticipating the probable tribological outcome for any given mechanical conditions under test.

Whilst *in-vitro* evaluation of new products is the *de-facto* standard for understanding wear behaviour and is often necessary for regulatory approval, this testing can be expensive and time consuming. In many cases, a high-speed, low cost computational prediction capability is an excellent ancillary tool to use in conjunction with the more physically substantiable results from *in-vitro* testing. For example, early screening of implant geometry design changes, or large-volume probabilistic or design-of-experiment studies can greatly aid development of novel designs. To this end, various researchers have applied *in-silico* wear prediction tools for computational models of the hip [2-6], knee [7-10], spine [11] and shoulder [12], amongst others.

The basis for the earliest implant wear algorithms was the work of Archard [13]. His tests were performed using metal pins on metal rotating rings and did not test orthopaedic-grade polymers, nor use multi-directional sliding. In its simplest derivative form, the Archard relationship may be expressed as:

$$W_d = k_A \cdot P \cdot S$$

where W_d is the wear depth, P the local contact pressure, S the magnitude of the sliding distance and k_A is the *Archard wear constant* - a constant of proportionality which must be empirically derived. The wear volume is then the sum integral of the localised wear depth across the wear area; it is hence easy to see how this model lends itself to application with computational numerical methods, which employ piecewise numerical discretisation of spatial and temporal variations. This model was first applied to orthopaedic implants (acetabular cups) by Maxian et al [3], and may be considered the baseline 'first generation' model from which all other subsequent models have been derived.

However, experimental evidence from both pin-on-disk (POD) tests [14] and implant tests [15, 16] soon suggested that other factors were complicit even within the limited domain of contact kinematics. Multi-directional sliding was theorised to produce high wear rates, due to the molecular long-chain structure of the polymer [17]. Theoretical models soon evolved to incorporate this concept, introducing the concept of cross-shear (CS); essentially, a measure of the intra-cycle deviation in sliding orientation relative to the principle sliding direction. To date, CS has been applied as a *cycle-averaged* measure of the variation in sliding direction, normalised to the path size. At a most basic level, it may be considered as representing the aspect ratio of the path, and indeed, in some papers the aspect-ratio is used as a simple surrogate CS metric [18]:

$$W_d = f(CS) \cdot P \cdot S$$

$$f(CS) = k_{CS} \cdot \frac{|ML|}{|AP|}$$

The *ML* and *AP* terms represent the sum magnitude of sliding in the medial-lateral (ML) and anterior-posterior (AP) directions. (The value of the wear constant, k_{CS}, will depend upon the formulation used for CS). However, it is possible to devise more elaborate permutations; for example Hamilton et al proposed an elegant crossing-intensity metric [19], and Willing proposed a geometrically-derived alternative [20]. We have previously demonstrated that, regardless of the precise format used to express CS, this family of second-generation algorithms have a comparable predictive power when benchmarked using a broad cohort of total knee replacement (TKR) tests [21], with moderate correlation coefficients ($R^2 \approx 0.6$ maximum) providing only a qualitative tool for design engineers and surgeons. This suggests that the current wear models could be improved further.

In this paper, we propose a fundamental re-evaluation of the representation of CS. Leaving aside the effect of kinetics, we will focus purely on *kinematics* (i.e. the sliding distance and CS terms in the wear algorithm). Recent POD test results [22] show that existing second generation models fail to predict wear under certain kinematic conditions when the assumption of constant wear within a cycle is not valid. This is because they use a simplified *cycle-averaged* determination of CS. The limitation of such an approach can be demonstrated by an abstract analysis, highlighting two key points:

Acausality: the first important point is that any cycle-averaged representation of CS is fundamentally acausal; it requires a prior knowledge of the final sliding path to predict the wear at the early stages of the cycle. Consider a path featuring a 90° turn late in the profile; clearly, this event cannot initially create high CS, until after the turn has occurred, but a cycle-averaged CS term inherently assigns a high wear factor across the entire profile, effectively making the model acausal. It has been proposed that this effect may be considered as a form of memory [23].

Scale-independence: the second point is that most second-generation wear algorithms will predict the same CS value (and hence the same wear-rate per unit sliding distance) for any geometrically similar path, regardless of scale. So a square path of side 20mm would be expected to generate ten times the wear of a square path of side 2mm (assuming no difference in other sliding parameters; e.g. lubrication or contact-pressure). In the extreme case, this leads to a logical inconsistency; an 'ultra-long' square side (e.g. several million mm) would not be expected to wear, as it is essentially a series of uni-directional sliding events, with a relatively insignificant proportion of turning events interspersed.

POD tests exploring this effect [22] demonstrated that wear increases with path scaling only for short distances, and then beyond a critical sliding distance, S_C (which appears to be on the order of a few mm), the wear does not appear to increase linearly as the path scaling is increased for larger distances; instead, the wear per turn tends towards a final value. The theorised characteristic response is illustrated in Figure 1.

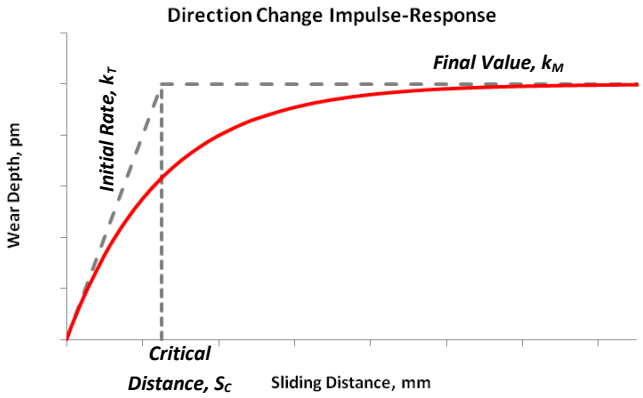

Figure 1: Impulse-response for wear versus sliding motion, following a step-change in sliding direction; based on concepts from [22].

From this response, the "corner point" (which corresponds to S_C) can be determined, using the steady-state wear depth, k_S, and the transient initial wear rate, k_T:

$$S_C = \frac{k_M}{k_T}$$

where S_C and k_M are in units of length, and k_T is dimensionless. Experimental results [22] show values for k_M and k_T vary depending upon the material (e.g. degree of polymer cross-linking).

As will be shown, determining k_M from experimental testing is relatively simple. Any test with a nominally 'long' distance between turns should approach close to the final value, k_M, per turn – so k_M is given simply by the ratio of total wear depth to number of turns for the duration of the test. On the other hand, k_T requires comparison of wear rates from multiple different tests with different sliding distances between turns – an exponential relationship can then be fitted to the ratio of wear rate versus sliding distance per turn.

This experimental evidence, combined with the analytical considerations outlined above, provides the basis for proposing a new framework for wear algorithms, which we term a 'third-generation' approach to differentiate from the existing family of second-generation CS-based methods.

Methods: Wear Theory

As in previous models, polyethylene wear is driven primarily by motion that is skewed to the principal sliding direction. However, unlike the earlier models which had no dependence on prior sliding, our proposed framework predicts wear by comparing the orientation of the current sliding direction to a history of previous sliding events. The instantaneous wear-depth at each time-step is added to the cumulative wear total, but also incorporated into an evolving polymer orientation.

Polymer Orientation and Polarization

The surface geometry of the polymer is discretised into elements, and the motion is also time-discretised such that each segment of the sliding path may be considered a linear translation having constant orientation. Then for each element, we establish a weighted time-history of its past sliding events via an accumulation of sliding vectors into a *Polar Vector Array* (PVA):

$$\begin{matrix}(\mu_1 & \phi_1)\\(\mu_2 & \phi_2)\\ \vdots & \\(\mu_i & \phi_i)\end{matrix}$$

where for each vector *i* in the array, the angle term ϕ_i (defined relative to the polymer co-ordinate system in polar coordinates) represents the recorded direction of *past* sliding events, and the magnitude term μ_i represents the relative 'strength' associated with that direction, such that:

$$\sum_i \mu_i = 1$$

So the polar-vector-array will always sum to a total strength of unity. New terms can only be added into the array by depreciating the existing values.

This concept may be illustrated with an example comparing a fully aligned orientation to one that is fully randomized (Figure 2). The fully polarised surface locality would have a single vector in the array, with magnitude μ = 1, and a single alignment ϕ corresponding to the orientation of the uni-directional sliding. A highly unpolarised locality, on the other hand, would have a large number of vector elements, each with a different ϕ value, and comparatively small individual magnitudes, but still summing up to 1.

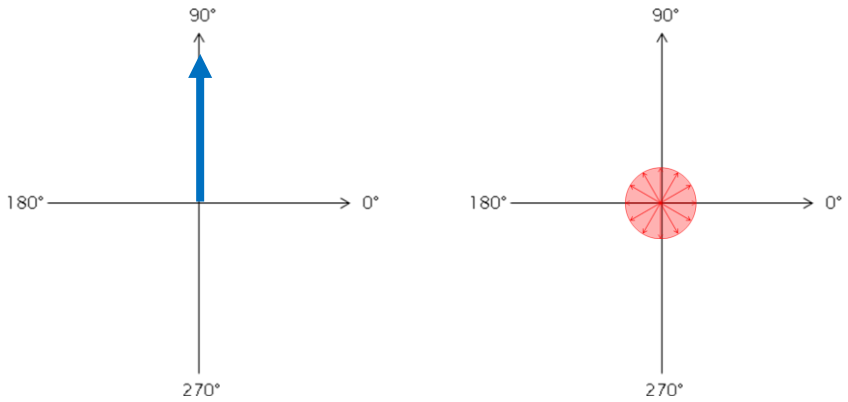

Figure 2: comparing a fully polarised PVA (left) with a perfectly apolar PVA (right). In practice, the distribution could take any shape, provided the vector magnitudes sum to unity.

Determining Wear

In general the wear depth, W_d, depends on the direction of motion (similar to cross-shear), pressure, and the amount of sliding:

$$W_d = k_M \cdot f(CS) \cdot f(P) \cdot f(S)$$

where k_M is an experimentally-derived constant which determines the maximum possible potential wear depth per step-turn. This value can be directly determined from POD tests[22], as the wear per turn divided by the pin area for a 90° turn event. Note that both the value and units of k_M can change depending upon *f(CS)*, *f(P)* and *f(S)*.

The terms *f(CS)*, *f(P)* and *f(S)* are generic functions for cross-shear, contact pressure and sliding distance respectively. We will provide specific relationships for *f(CS)* and *f(S)*, but will not advocate any single relationship for *f(P)*, as the form of this dependency is still debated.

f(CS): the wear due to a sliding event with distance *S* and direction θ will be governed by a *surface potential* that we term ζ (this essentially acts as the equivalent to the 'cross-shear' function *f(CS)* in second-generation algorithms):

$$\zeta = \sum_i \mu_i \cdot \left|\sin(\theta - \phi_i)\right|$$

where μ_i and ϕ_i are the vector quantities of the orientation stored in the PVA. Note that the magnitude of the sine evaluation is used, reflecting the common assumptions that components of motion orthogonal to orientation contribute to wear but components parallel to orientation (uni-directional or reciprocating sliding paths) do not contribute appreciably to wear [17]. By inspection, it can be seen that ζ must lie between 0 and 1. The maximum value can only occur if the current PVA is fully polarised in a direction perpendicular to θ. If the sliding occurs parallel to a fully polarised PVA (i.e. uni-directional or reciprocating motion where $\phi = \theta$) then ζ is zero. With decreasing polarisation, ζ will tend towards a mid-range value, and for a totally unpolarised surface, (when the PVA describes a circle), $\zeta = 0.5$).

f(P): while early wear models assumed a linear proportionality between wear and contact pressure, important work by subsequent researchers has challenged this assumption [24-30]. Therefore this framework allows for alternative formulations to be used. Researchers are encouraged to evaluate the evidence in the literature to determine their approach (there is some evidence that this *f(P)* function may be relatively small in effect, compared to the motion paths [21]; so differences may not be large).

f(S): at the simplest level, a straightforward linear proportionality may be applied for sliding distance, and for very fine step sizes this is perfectly adequate. However recent data suggests a variable wear for long sliding distances [22] so for larger sliding distance steps, it is necessary to compensate for the re-polarisation occurring *within* the time step. This can be done with an exponential expression:

$$f(S) = 1 - e^{-S \cdot \frac{k_T}{k_M}}$$

Where k_T is a *transient* constant, which determines the rate at which this exponential term decays. This value can be derived from experimental data and is also dependent upon the specific algorithm formulation. It is possible to express *f(s)* in terms of the critical sliding distance S_C:

$$S_C = \frac{k_M}{k_T} \qquad \text{such that:} \qquad f(S) = 1 - e^{-\frac{S}{S_C}}$$

It may be verified that for small step-sizes, both values converge to give identical results, and in the final algorithm a sequence of fine steps using the simpler proportional model will yield the same decrease in wear rate with progressive sliding. For this reason researchers are encouraged to use the nonlinear approach (although individual steps are slightly more computationally expensive to

evaluate in this latter permutation, the step size can potentially be increased to compensate, reducing the number of for example FEA simulation steps required).

One final quantity must be defined before proceeding; the *maximum potential wear depth*, W_p:

$$W_p = k_M \cdot \zeta \cdot f(P)$$

W_p is the wear depth which would ensue with an unlimited amount of sliding in the θ direction. The actual wear depth, W_d will typically be less than W_p, since the sliding distance per step will be limited; the ratio between W_d and W_p is used to evolve the PVA ready for the next time-step.

Modifying the Polarisation Vector Array

To demonstrate how the surface polarisation, as described by the PVA, changes in time consider a new sliding event at the next time-step with sliding distance *S* and direction θ. This new sliding will modify the past sliding history recorded in the PVA according to a *strength modifier*, denoted λ:

$$\lambda = \frac{W_d}{W_p}$$

Note that if the step-size is too large, it may not be valid to assume that wear is constant across the step; in this case, limit-checking may be used to ensure that the calculated value of W_d does not exceed the permitted maximum, W_p; i.e. $\lambda \leq 1$. If the exponential form for *f(S)* is used then λ can never exceed 1.

This λ value is used to scale down the strength of all elements in the existing PVA:

$$\mu_i = \mu_i(1-\lambda)$$

And then, subsequently, to add a new element (*i+1*) to the array, to represent the polarising effect of the current sliding step in the direction theta:

$$\phi_{i+1} = \theta$$

$$\mu_{i+1} = \lambda$$

such that the sum of all μ values is always inherently constrained to unity. At this point, one iteration of the algorithm is complete, and the next iteration begins with a new initial PVA, new time-step values for θ, *S*, *P*, etc.

Note that the number of vectors in the PVA will tend to grow over time, progressively slowing evaluation. One possibility is to scan for and remove vectors with a low μ-value below a user-specified threshold, e.g. 0.001 (if this is done, the remaining vector elements must be scaled up accordingly). An alternative solution is to collate the PVA vectors into a series of 'bins' spanning the full angular range (0 - 360°); more bins give greater accuracy but a larger array, hence slower execution. Sensitivity studies (not described, for brevity) suggest that a good trade-off is a bin size of ~3°, giving an upper limit of 120 elements in the PVA.

This algorithm must be evaluated for each location on the articulating contact surface, at each point in time. The driving input data may be sourced from computational models of the mechanical set-up (e.g. finite-element, multi-body dynamics, or purely analytic).

Note that some initial value is needed for the polarisation at time $t = 0$; there are two reasonable approaches:

- One option is to use a surrogate value based on 2nd-generation methods. For example, using the crossing intensity method proposed by Hamilton et al [19] to evaluate a weighted mean sliding direction $\overline{\theta}$, and using this value as the initial surface polarisation.

- Because the critical distance S_C is only a few mm (less than the typical sliding per gait-cycle), the other option is to assign an arbitrary value to the PVA, and then run one or more iterations of the algorithm to pre-condition the array (without storing wear depths), then a subsequent iteration for the actual wear calculations. This is simpler, but requires additional execution time. If the path length is significantly greater than S_C at most contact locations, then the first iteration may provide a sufficiently close approximation even without pre-loading the PVA. Conversely, if the path length is very short, it may be advisable to use a conditional loop, repeatedly iterating until the predictions converge to within acceptable tolerances.

Figure 3 summarises the algorithm described above in flow-chart form. Clearly, this framework is more complex than for example the 'aspect-ratio' estimate, and cannot be estimated without computational assistance. Given a discretised representation of the test kinematics and kinetics, it can however readily be implemented in any of a wide range of programming languages (a more text-based form of pseudocode is provided in appendix 1, which readers should be able to implement in a language of their choosing).

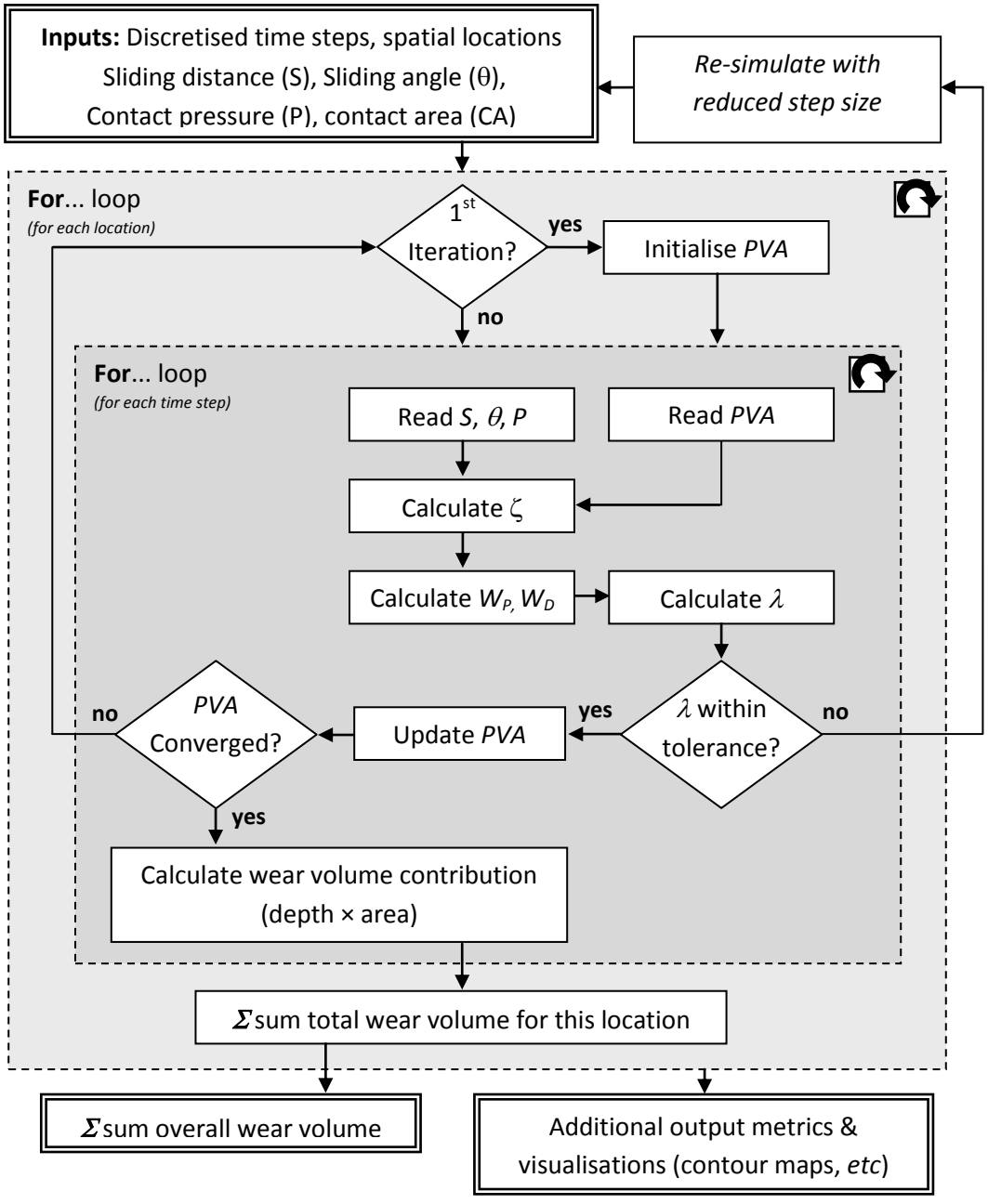

Figure 3: Algorithm describing the execution of the new wear model.

Implementation:

A version of this algorithm was encoded in MATLAB, and supplied with data based on basic POD profiles, and with a more complex data set from a single multi-body dynamics (MBD) model of a TKR wear test [31], and from a larger multi-cohort dataset [21]. This implementation of the algorithm set the contact-pressure sensitivity to zero (as proposed by Ernsberger et al [29] and previously implemented with limited impact on wear outcomes [21]), and used the more precise exponential-form for the sliding-distance term. The constants were determined using published results [22] for moderately-crosslinked UHMWPE: k_M = 18.2pm and k_T =12.3 pm.mm^{-1} (such that $S_C \approx$ 1.5mm). For a less crosslinked polymer, the constants were different (k_M = 45.5pm and k_T =18.2 pm.mm^{-1}), reinforcing the fact that any model is material-specific. Interestingly, in both cases the value of k_M must be on the sub-angstrom scale to match the experimentally-observed average depth per turn.

For the internal parameters, around 200 time-steps were used to represent the gait cycle for TKR tests, with a higher resolution (2000 time-steps) for the idealised POD profiles. The PVA bin tolerance was set to 3°, and 3 recursive iterations were used to ensure that the final cycle used a fully pre-conditioned PVA (removing transient first-cycle artefacts).

The evaluation time for the POD profiles was negligible (milliseconds), and ~10 seconds for the full TKR gait profile (~200 time steps, ~600 individual contact locations). This is low enough for most general deterministic modelling, but may be significant for adaptive probabilistic modelling, where thousands of repeated iterations may be used [32]. Therefore, the performance-accuracy trade-offs discussed above could become important.

POD Applications: Idealised Analytic Paths

The first validation exercise was to demonstrate that the proposed algorithm could match the predictions of POD tests [22]. To this end, a series of idealised single-location input vectors were devised, to simulate reciprocal sliding followed by a sudden 90° step-change in direction, with different sliding distances between turns. Figure 4 shows the predicted intra-cycle instantaneous wear rate following a single turn; note that for the shortest distances, the PVA never becomes fully re-oriented before the next turn (hence peak wear never reaches the transient value of k_T; for the highest distances the wear rate quickly drops off to negligible levels (such that further sliding does not contribute to wear).

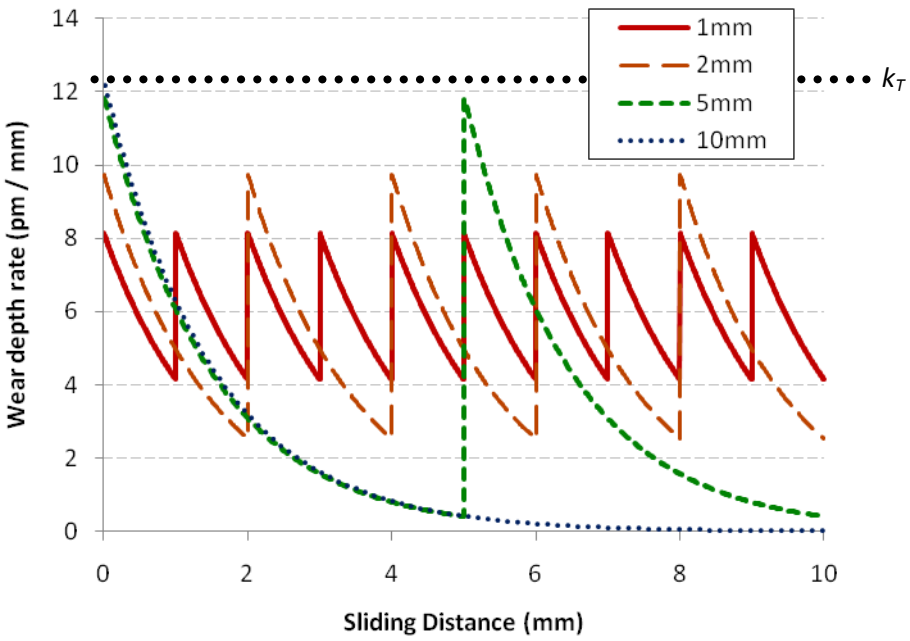

Figure 4: Intra-cycle wear rates for different turn tests (100mm not shown due to scale).

Figure 5 shows the comparison versus results from [22]. Results show reasonable agreement with the experimental trends, given the *in-vitro* variability.

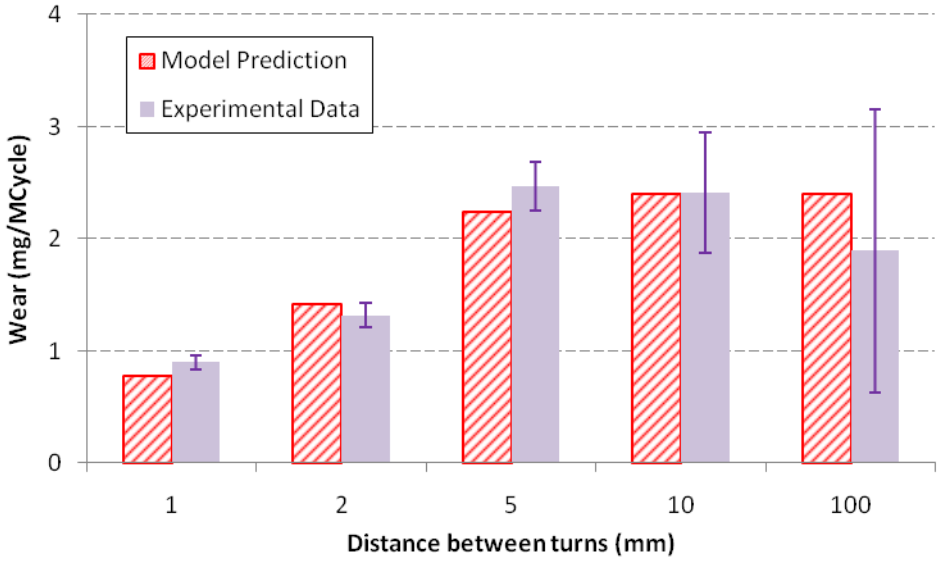

Figure 5: Comparison of published experimental POD test data for crosslinked UHMWPE [22] versus corresponding computational predictions using new 3rd generation algorithm.

Because this algorithm is scale-dependent, it is difficult to compare to the idealised analytic predictions of other extant models. To illustrate this scale-dependence, in appendix 2 the algorithm is compared to other approaches, at a range of different scales.

Implant Wear Applications: Assessing predictive power versus larger test cohort:

We have previously reported a large-cohort study used to determine the predictive power of 1st- and 2nd-generation algorithms, in which we found that the best predictive power of extant models was around R^2=0.60 [21]. Using the new 3rd-generation algorithm we re-visited this dataset, using the same mechanical outputs as in the previous paper, and using the above POD-derived coefficients within the algorithm. The result is shown in Figure 6. There is a limited increase in the predictive power of the algorithm (from ~0.60 to ~0.65), although this improvement is small. However, the constant of proportionality is 0.90; close to unity, implying the outputs are quantitatively, and not just qualitatively, meaningful (i.e. the POD results translate well into the TKR tests).

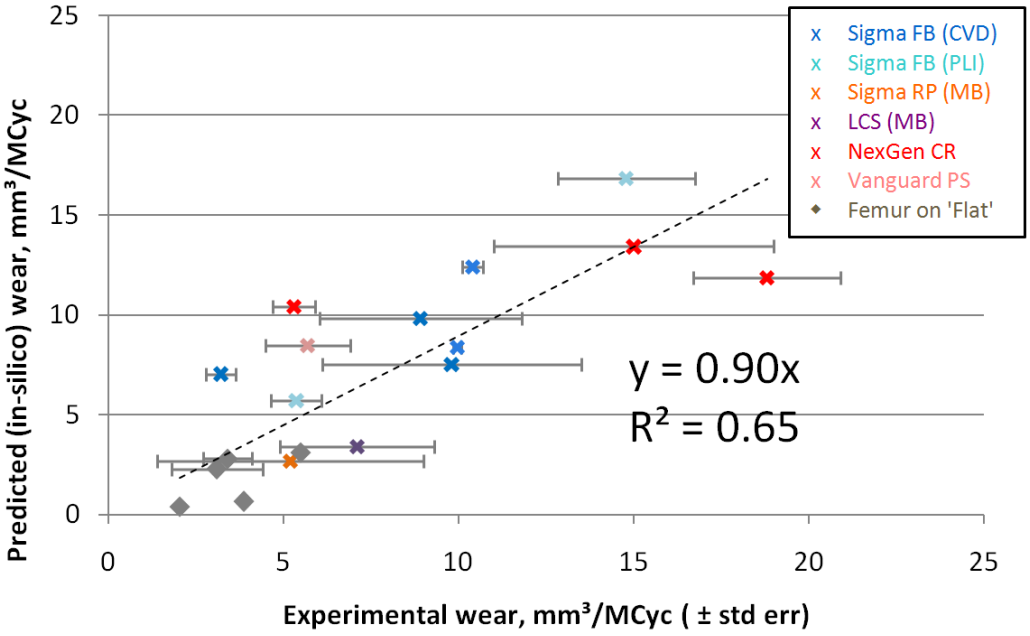

Figure 6: 3rd generation algorithm performance: comparison with large-cohort experimental data from [21].

Discussion:

In this paper, we have presented a generic, flexible framework for better modelling the effect of kinematics upon wear. We have outlined the steps in the proposed algorithm and demonstrated a simple implementation in MATLAB. We have illustrated how this algorithm can match predictions from recent POD tests, and that the coefficients derived from POD testing provide encouragingly good quantitative predictions when mapped to TKR wear tests.

This new algorithm does represent an increase in complexity and corresponding computational overhead, but this increase in complexity is necessary to account for the reported results of recent experimental POD testing. To mitigate, several means to tune the performance-accuracy trade-off have been described, so the increase in overhead may be tailored according to specific applications.

Note that here we propose a generic *framework*; hence we have attempted to avoid being too prescriptive in areas where academic opinion remains divided; most particularly with regards to the influence of contact pressure on wear rates. Whilst the traditional view has been that wear increases with pressure, some POD test results have suggested that wear is either independent of pressure, increasing instead according to contact area [29, 30], or even that wear may be inversely related to

pressure [28]. Nonetheless evidence from TKR tests would still seem to suggest that very high contact stresses can increase wear [33]. Given this split of evidence, we do not at this time attempt to prescribe one solution as correct, but leave this issue open within the framework for researchers to follow their preference. At present our own approach, based on the limited sensitivity to contact pressure shown by previous studies [21], is to discount the pressure-term, unless considering data for unusual tests outside the usual range of observed conditions (e.g. with low-conformity 'flat' implants).

Still, an important limitation here is the scope of this wear model. Many factors and influences remain relatively underexplored and are not accounted for in virtual wear prediction tools. In this paper, we have not addressed the highly important issue of incorporating additional factors. For example, investigators have reported early attempts to account for additional effects within contact mechanics, (such as the effect of cyclic or intermittent contact [34], or the mechanics associated with three-body wear [35]) and a wide range of other factors (temperature, fatigue, etc) remain to be modelled. Here instead we have focused on the conventional domain of contact kinematics. However, we have attempted to present this work in a generic architecture, which could very readily be augmented to include further factors; so this work is complementary to ongoing efforts to expand the scope of wear modelling to include novel factors. The inclusion of such additional terms may help to more explicitly model the influence of parameters such as contact-pressure which are currently not entirely resolved, and should be an important primary goal for next-generation algorithms. This may require a combination of both empirical and mechanical modelling on both the macro-and micro-scale.

At the implant-level, the behaviour of the model is comparable to existing approaches, the predictive power of the new algorithm versus implant tests is not substantially greater; however, this is to be expected, for two reasons. Firstly, as discussed above, the model is not exhaustive in its scope; there are other factors (material variations, other wear mechanisms, etc) which could be incorporated. Secondly, the experimental variability itself is still very large; fundamentally achieving a better correlation coefficient requires either that the experimental variability of the data-set be lower (by improved experimental procedure), or that the variability be accounted for within the computational domain (e.g. by stochastic modelling). An important conclusion from this is that without a wider body of comparable experimental data, further improvements in theoretical models of wear will be limited. Coefficient values are reported here for two grades of UHMWPE, with different levels of cross-linking. Different values for different grades have also been reported by other investigators [36], and generally, the constants should be tuned to the particular polymer grade under test (the values we report for conventional versus crosslinked polymers differ by more than a factor of two). Validating any tribological model is difficult, since wear experimentation is challenging; this is compounded here because the theory anticipates very short-timescale changes in the polymer response (within a few mm of sliding); this cannot be directly measured for an individual cycle, so inferences have been drawn from cycle-averaged estimates. This derivation involves inherent assumptions (e.g. that the wear per cycle is relatively consistent). Further, the model is based on limited data points (e.g. very short, sub-millimetre paths could not be generated to populate the nonlinear region in figure 4). Further testing is still much needed to explore some of the secondary effects and alternative mechanisms which are currently not prescribed within the framework.

No discussion is made in this paper of adaptive wear methods (e.g. [9, 37]) or creep modelling [7, 38], to avoid complicating the introduction of the new algorithm. We note that there is nothing within the proposed framework which is incompatible with such methods, and they could easily be incorporated within and around this outline algorithm. Obviously, such important factors must ultimately be accounted for as part of the holistic perspective of next-generation wear prediction-tools.

Evidently, any computational predictive tool for wear can only be as good as the mechanical model it is based on; where finite-element or MBD-based models are used to supply the discretised data for these algorithms, it is essential that those models too are well-validated and high-integrity (holistic modelling based on extensive experimental data and using appropriate statistical modelling methods [39]).

We believe that there is excellent potential to advance the science of implant wear prediction, and we submit these methodologies in the hope that they will be assistive in furthering *in-silico* wear modelling and prediction capabilities across the research and design community.

Acknowledgements:

This research has been supported by the Engineering and Physical Sciences Research Council (EPSRC) UK. Modelling support has been provided by DePuy, a Johnson & Johnson company.

Appendix 1: representative pseudocode for wear algorithm

```
// 3G Wear Algorithm Generic Pseudocode (M.A. Strickland, U.Southampton)

// INPUT PROFILE VARIABLES
n = 2000              // Number of path-steps to simulate
dist = 20             // total sliding distance (mm)
s(1:n) = dist/n       // sliding distance per path-step (mm)
CP(1:n) = 1           // CP term held 'fixed' this demonstration

// PICK A GENERIC 'PATH' BY COMMENTING IN/OUT ONE OF THE OPTIONS BELOW:
//1. uni-directional sliding:
  // theta(n) = 0     // path segment angle, in degrees (°)
//2. bi-directional sliding (single inversion midway):
  // theta(1:n/2) = 0
  // theta(n/2+1:n) = 180°
//3. single 90° turn ("impulse response"):
  // theta(n) = 90°
//4. constant rotation (circles):
  theta(1:n) = 0:360°

theta = limits(0, 360°)    // limit angles to range 0° to 360°

// wear depths/constants in picometres (10^-12m) to avoid floating-point issues.
kt = 18.2             // 'transient' constant (initial wear rate); units: pm/mm
km = 45.5             // 'maximum' constant (final wear level); units: pm
Sc = km/kt            // 'critical' (or 'corner') sliding distance, mm
PVA = {1,0}           // initialise the polar-vector array. Format: {mu, phi}
bin_tol = 1°          // 'bin' size for the PVA, 'tolerance' (in degrees).
loops = 3             // how many loops to set an appropriate value for the PVA

for loop (l = 1 to loops)  // may use loops to pre-set PVA initial value...
  wd(1:n) = 0   // Instantaneous wear depth contributions (pm)
  for loop (i = 1 to n)      // for each time step:
    zeta(1:n) = sum( PVA{1:n,1} * abs(sin(theta(i) - PVA{1:n,2})) )
    wp = km*zeta*CP(i)                          // 'full' potential sliding effect
    wd(i) = km*zeta*CP(i)*(1-exp(-s(i)/Sc)) // actual effect (given 's')

    if condition (wd(i)>0 and wp>0) // only update PVA if any wear has occurred
      lambda = wd(i)/wp          // strength modifier increment
      if condition (lambda > 0.1)  // low sample rate warning (>10% change in PVA)
        message('warning: large changes per step; increase sample rate')
      ...end if condition
      // update the PVA; scale 'magnitude' term for all existing elements:
      PVA{:,1} = PVA{:,1} * (1-lambda)
      // Add to PVA; use existing element ('bin') if possible:
      if condition (bin_tol == 0°) // requires exact match
        imatch = findmatch(PVA{:,2}, theta(i)) // try to find existing match in PVA
      else // needs only to be within tolerance (use 'bin_tol'):
        imatch = findmatch(round(PVA(:,2)/bin_tol), round(theta(i)/bin_tol))
      ...end if condition

      if condition (imatch <> 0) // if match found, augment that existing element:
        PVA{imatch,1} = PVA{imatch,1} + lambda
      else // if there was no match, then append a new row:
        PVA = append(PVA, {lambda, theta(i)})
      ...end if condition

    ...end if condition

  ...end for loop

...end for loop

w_total = sum(wd)  // sum contributions from each path-step to get overall wear
```

Appendix 2: Comparison vs. existing wear predictors

The proposed model in this manuscript anticipates a decreasing wear per unit sliding distance as the path-scale increases; whereas, previous 2nd generation models (from Turell et al [14] and Hamilton et al [19]) predict no difference (Figure A1). To reinforce this point, we have contrasted their performance at various scale lengths (Figure A1) and shapes (Figure A2). From a mathematical perspective, the decline in wear per unit sliding (Figure A1) can be derived by taking the derivative of the exponential relationship of wear depth (Figure 1). Note the previous models were not scale-dependent, therefore results are normalised so that the very shortest path-length is considered to have a wear per unit sliding distance of 100%.

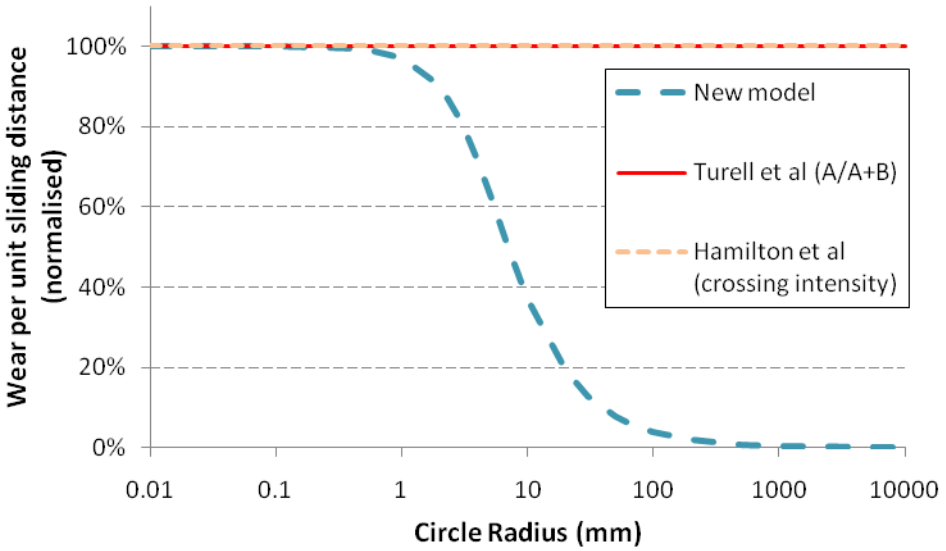

Figure A1: comparison of predicted wear per unit sliding distance for circle paths of varying radius.

In regard to predicting wear for different shapes, the general trends are common among the different formulations (Figure A2). It is important to note that these comparisons have been performed using a fixed path length (20mm) with a 20mm circumference circle as worst case (unity wear factor). If, however, a different path-length had been chosen, the relative values for the new model could change dramatically as seen in the case of a circle described above (Figure A2).

Shape	A/A+B[14]	σ*[19]	New Model		Shape	A/A+B[14]	σ*[19]	New Model
circle (=100%)	100%	100%	100%		*Ellipse, e=0.661*	86%	82%	97%
	100%	87%	76%			67%	59%	86%

90° rhombus					*Ellipse, e=0.866*			
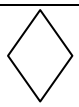 *60° rhombus*	73%	58%	65%		 *Ellipse, e=0.968*	40%	30%	57%
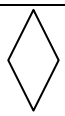 *30° rhombus*	42%	29%	38%		 *Ellipse, e=0.995*	18%	12%	26%
 *10° rhombus*	16%	10%	13%		*Ellipse, e=0.999*	10%	6%	14%
bi-directional	0	0	0					

Figure A2: Comparison of predicted wear (normalised to 'worst-case' circle) for different path shapes (total path length = 20mm).

References:

1. Green, T.R., et al., *Polyethylene particles of a 'critical size' are necessary for the induction of cytokines by macrophages in vitro.* Biomaterials, 1998. **19**(24): p. 2297-2302.
2. Wu, J.S.-S., et al., *The computer simulation of wear behavior appearing in total hip prosthesis.* Computer Methods and Programs in Biomedicine, 2003. **70**(1).
3. Maxian, T.A., et al., *3-Dimensional sliding/contact computational simulation of total hip wear.* Clin Orthop Relat Res, 1996(333): p. 41-50.
4. Kang, L., et al., *Quantification of the effect of cross-shear on the wear of conventional and highly cross-linked UHMWPE.* J Biomech, 2008. **41**(2): p. 340-6.
5. Matsoukas, G. and I.Y. Kim, *Design Optimization of a Total Hip Prosthesis for Wear Reduction.* Journal of Biomechanical Engineering, 2009. **131**(5): p. 051003-12.
6. Liu, F., et al., *A new formulation for the prediction of polyethylene wear in artificial hip joints.* Proceedings of the Institution of Mechanical Engineers, Part H: Journal of Engineering in Medicine, 2010. **224**.
7. Willing, R. and I.Y. Kim, *A holistic numerical model to predict strain hardening and damage of UHMWPE under multiple total knee replacement kinematics and experimental validation.* Journal of Biomechanics, 2009. **42**(15): p. 2520-2527.
8. Fregly, B.J., et al., *Computational wear prediction of a total knee replacement from in vivo kinematics.* J Biomech, 2005. **38**(2): p. 305-14.
9. Knight, L.A., et al., *Comparison of long-term numerical and experimental total knee replacement wear during simulated gait loading.* J Biomech, 2007. **40**(7): p. 1550-8.
10. Zhao, D., et al., *Predicting Knee Replacement Damage in a Simulator Machine Using a Computational Model With a Consistent Wear Factor.* Journal of Biomechanical Engineering, 2008. **130**(1): p. 011004-10.
11. Goreham-Voss, C.M., et al., *Cross-shear implementation in sliding-distance-coupled finite element analysis of wear in metal-on-polyethylene total joint arthroplasty: Intervertebral total disc replacement as an illustrative application.* Journal of Biomechanics, 2010. **43**(9): p. 1674-1681.
12. Hopkins, A.R., et al., *Wear in the prosthetic shoulder: association with design parameters.* J Biomech Eng, 2007. **129**(2): p. 223-30.
13. Archard, J.F., *Contact and Rubbing of Flat Surfaces.* Journal of Applied Physics, 1953. **24**(8): p. 981-988.
14. Turell, M., A. Wang, and A. Bellare, *Quantification of the effect of cross-path motion on the wear rate of ultra-high molecular weight polyethylene.* Wear, 2003. **255**(7-12): p. 1034-1039.
15. McEwen, H.M.J., et al., *Wear of fixed bearing and rotating platform mobile bearing knees subjected to high levels of internal and external tibial rotation.* Journal of Materials Science: Materials in Medicine, 2001. **12**(10-12): p. 1049-1052.
16. Bragdon, C.R., et al., *The importance of multidirectional motion on the wear of polyethylene.* Proc Inst Mech Eng H, 1996. **210**(3): p. 157-65.
17. Wang, A., *A unified theory of wear for ultra-high molecular weight polyethylene in multi-directional sliding.* Wear, 2001. **248**(1-2): p. 38-47.
18. Knight, L.A., et al. *Influence of cross shear on the wear of TKA under various kinematic conditions*. in *52nd Annual Meeting of the Orthopaedic Research Society*. 2006. Chicago, USA: Orthopaedic Research Society.
19. Hamilton, M.A., et al., *Quantifying multidirectional sliding motions in total knee replacements.* ASME. Journal of Tribology, 2005. **127**(2): p. 280-6.
20. Willing, R.T. and I.Y. Kim, *A Pseudo-Qualitative Method for Measuring Cross-Shearing motions in Total Knee Replacements*, in *Transactions of the 54th Annual Meeting, Orthopaedic Research Society* 2008: San Francisco, CA.
21. Strickland, M.A. and M. Taylor, *In-silico wear prediction for knee replacements - methodology and corroboration.* Journal of Biomechanics, 2009. **42**(10): p. 1469-1474.

22. Dressler, M.R., et al., *Predicting wear of UHMWPE: Decreasing wear rate following a change in direction.* Wear, 2011. **271**(11-12): p. 2879-2883.
23. Petrella, A., et al., *A Generalized Model for Cross-Shear Wear in Joint Replacements*, in *Transactions of the 55th Annual Meeting, Orthopaedic Research Society* 2009: Las Vegas, NV.
24. Vassiliou, K. and A. Unsworth, *Is the wear factor in total joint replacements dependent on the nominal contact stress in ultra-high molecular weight polyethylene contacts?* Proceedings of the Institution of Mechanical Engineers, Part H: Journal of Engineering in Medicine, 2004. **218**(2): p. 101-107.
25. Barbour, P.S.M., D.C. Barton, and J. Fisher, *The influence of contact stress on the wear of UHMWPE for total replacement hip prostheses.* Wear, 1995. **181-183**(Part 1): p. 250-257.
26. Saikko, V., *Effect of contact pressure on wear and friction of ultra-high molecular weight polyethylene in multidirectional sliding.* Proceedings of the Institution of Mechanical Engineers, Part H: Journal of Engineering in Medicine, 2006. **220**(7): p. 723-731.
27. Wang, A., A. Essner, and R. Klein, *Effect of contact stress on friction and wear of ultra-high molecular weight polyethylene in total hip replacement.* Proc Inst Mech Eng H, 2001. **215**(2): p. 133-9.
28. Kang, L., et al., *Enhanced computational prediction of polyethylene wear in hip joints by incorporating cross-shear and contact pressure in additional to load and sliding distance: Effect of head diameter.* Journal of Biomechanics, 2009. **42**(7): p. 912-918.
29. Ernsberger, C., D. Whitaker, and J. Chavarria, *UHMWPE Wear Rate As A Function Of Contact Area And Stress*, in *Transactions of the 53rd Annual Meeting, Orthopaedic Research Society* 2007: San Diego, CA.
30. Mazzucco, D. and M. Spector, *Effects of contact area and stress on the volumetric wear of ultrahigh molecular weight polyethylene.* Wear, 2003. **254**(5-6): p. 514-522.
31. Strickland, M.A., M. Browne, and M. Taylor, *Could passive knee laxity be related to active gait mechanics? An exploratory computational biomechanical study using probabilistic methods.* Computer Methods in Biomechanics and Biomedical Engineering, 2009. **12**(6): p. 709-20.
32. Strickland, M.A., et al., *A multi-platform comparison of efficient probabilistic methods in the prediction of total knee replacement mechanics.* Comput Methods Biomech Biomed Engin, 2010. **13**(6): p. 701-9.
33. Grupp, T.M., et al., *Fixed bearing knee congruency -- influence on contact mechanics, abrasive wear and kinematics.* Int J Artif Organs, 2009. **32**(4): p. 213-23.
34. Strickland, M.A. and M. Taylor, *Analysing 'Lift-off' Events During Knee Wear Testing*, in *European Society of Biomechanics*. 2010: Edinburgh, UK.
35. Cenna, A.A., et al., *Modelling the three-body abrasive wear of UHMWPE particle reinforced composites.* Wear, 2003. **254**(5-6): p. 581-588.
36. Korduba, L.A., et al., *How Much Does Cross-Path Motion Matter In The Wear Of Polyethylene?*, in *Transactions of the 56th Annual Meeting, Orthopaedic Research Society* 2010: New Orleans, LA.
37. Maxian, T.A., et al., *Adaptive finite element modeling of long-term polyethylene wear in total hip arthroplasty.* J Orthop Res, 1996. **14**(4): p. 668-75.
38. Lee, K.-Y. and D. Pienkowski, *Compressive creep characteristics of extruded ultrahigh-molecular-weight polyethylene.* Journal of Biomedical Materials Research, 1998. **39**(2): p. 261-265.
39. Strickland, M.A., et al., *Targeted Computational Probabilistic Corroboration of Experimental Knee Wear Simulator: The Importance of Accounting for Variability* Medical Engineering & Physics, 2011. **33**(3): p. 295-301.